Dear author,

Please note that changes made in the online proofing system will be added to the article before publication but are not reflected in this PDF.

We also ask that this file not be used for submitting corrections.

Case Study

Neuron

Biomimetic Intraneural Sensory Feedback Enhances Sensation Naturalness, Tactile Sensitivity, and Manual Dexterity in a Bidirectional Prosthesis

Highlights

- Biomimetic hybrid sensory encodings are perceived as highly natural
- Biomimetic hybrid sensory encodings restore rich tactile sensitivity
- Biomimetic hybrid sensory encodings improve manual dexterity and accuracy
- Biomimetic hybrid sensory encodings enhance prosthesis embodiment

Authors

Giacomo Valle, Alberto Mazzoni, Francesco Iberite, ..., Francesco Maria Petrini, Paolo Maria Rossini, Silvestro Micera

Correspondence

silvestro.micera@epfl.ch

In Brief

Sensory encoding strategies are used to convey sensory information to upper limb amputees. Valle et al. present strategies based on biomimetic approaches that improve sensation naturalness, tactile sensitivity, manual dexterity, and prosthesis embodiment.

Valle et al., 2018, Neuron *100*, 1–9
October 10, 2018
https://doi.org/10.1016/j.neuron.2018.08.033

CellPress

Please cite this article in press as: Valle et al., Biomimetic Intraneural Sensory Feedback Enhances Sensation Naturalness, Tactile Sensitivity, and Manual Dexterity in a Bidirectional Prosthesis, Neuron (2018), https://doi.org/10.1016/j.neuron.2018.08.033

Neuron
Case Study

Biomimetic Intraneural Sensory Feedback Enhances Sensation Naturalness, Tactile Sensitivity, and Manual Dexterity in a Bidirectional Prosthesis

Giacomo Valle,[1,2] Alberto Mazzoni,[2] Francesco Iberite,[2] Edoardo D'Anna,[1] Ivo Strauss,[1,2] Giuseppe Granata,[3] Marco Controzzi,[2] Francesco Clemente,[2] Giulio Rognini,[1,4] Christian Cipriani,[2] Thomas Stieglitz,[5] Francesco Maria Petrini,[1,6] Paolo Maria Rossini,[3,6] and Silvestro Micera[1,2,7,*]

[1]Bertarelli Foundation Chair in Translational Neuroengineering, Centre for Neuroprosthetics and Institute of Bioengineering, School of Engineering, École Polytechnique Fédérale de Lausanne (EPFL), Lausanne CH-1202, Switzerland
[2]Center for Neuroscience, Neurotechnology, and Bioelectronic Medicine and BioRobotics Institute, Scuola Superiore Sant'Anna, Pisa 56025, Italy
[3]Institute of Neurology, Catholic University of The Sacred Heart, IRCCS-Policlinic A. Gemelli Foundation, Rome 00168, Italy
[4]Laboratory of Cognitive Neuroscience, Brain Mind Institute, Ecole Polytechnique Fédérale de Lausanne, Lausanne CH-1015, Switzerland
[5]Laboratory for Biomedical Microtechnology, Department of Microsystems Engineering–IMTEK, Bernstein Center, BrainLinks-BrainTools Cluster of Excellence, University of Freiburg, Freiburg D-79110, Germany
[6]These authors contributed equally
[7]Lead Contact
*Correspondence: silvestro.micera@epfl.ch
https://doi.org/10.1016/j.neuron.2018.08.033

SUMMARY

Peripheral intraneural stimulation can provide tactile information to amputees. However, efforts are still necessary to identify encoding strategy-eliciting percepts that are felt as both natural and effective for prosthesis control. Here we compared the naturalness and efficacy of different encoding strategies to deliver neural stimulation to trans-radial amputees implanted with intraneural electrodes. Biomimetic frequency modulation was perceived as more natural, while amplitude modulation enabled better performance in tasks requiring fine identification of the applied force. Notably, the optimal combination of naturalness and sensitivity of the tactile feedback can be achieved with "hybrid" encoding strategies based on simultaneous biomimetic frequency and amplitude neuromodulation. These strategies improved the gross manual dexterity of the subjects during functional task while maintaining high levels of manual accuracy. They also improved prosthesis embodiment, reducing abnormal phantom limb perceptions ("telescoping effect"). Hybrid strategies are able to provide highly sensitive and natural percepts and should be preferred.

INTRODUCTION

Grasping is a sophisticated activity that is pivotal for body-environment interaction. Therefore, re-establishing the sensory flow of information between hand prostheses and the brain is of paramount importance. Lack of sensory feedback and inadequate embodiment are among the reasons for rejection of available commercial prosthesis (Wijk and Carlsson, 2015).

Implantable peripheral nerve interfaces can be reliably used to provide sensory feedback to upper limb amputees (Graczyk et al., 2016; Horch et al., 2011; Ortiz-Catalan et al., 2014; Raspopovic et al., 2014, 2017; Tan et al., 2014, 2015). This approach can improve hand prosthesis movement control (Tan et al., 2014, 2015), is usable and stable over long periods (Ortiz-Catalan et al., 2014; Tan et al., 2015), and fosters embodiment of the prosthesis by the subjects (Rognini et al., 2018; Schiefer et al., 2016). Previous works also showed that different encoding strategies could be used to successfully restore sensory feedback (Graczyk et al., 2016; Horch et al., 2011; Tan et al., 2014, Wendelken et al., 2017). In particular, in these studies the amplitude or frequency of the injected stimuli was modulated (Horch et al., 2011; Raspopovic et al., 2014; Tan et al., 2014, Wendelken et al., 2017), eliciting somatotopic sensations (e.g., referred to phantom hand) with feelings that are sometimes similar to the natural ones (e.g., pressure or vibration). However, naturalness can be characterized by different "grades" and the "level" of naturalness has been often reported by the subjects as quite limited (e.g., using the stimulation is quite unpleasant; see, for example, Tan et al., 2014). Ideally, neural stimulation should be able to provide sensory feedback that is functionally effective and highly natural, as the naturalness of the feedback plays a pivotal role in prostheses acceptance (Graczyk et al., 2016; Saal and Bensmaia, 2015).

A possible way to address this issue might be to define and use complex stimulation patterns (Graczyk et al., 2016; Pasluosta et al., 2018; Tyler, 2015) that resemble the natural encoding strategies implemented by the nervous system (Chortos et al., 2016; Johansson and Flanagan, 2009). Here, to understand how to develop a more natural and informative encoding strategy for the control of the bidirectional prosthesis, we tested four different stimulation approaches (STAR Methods;

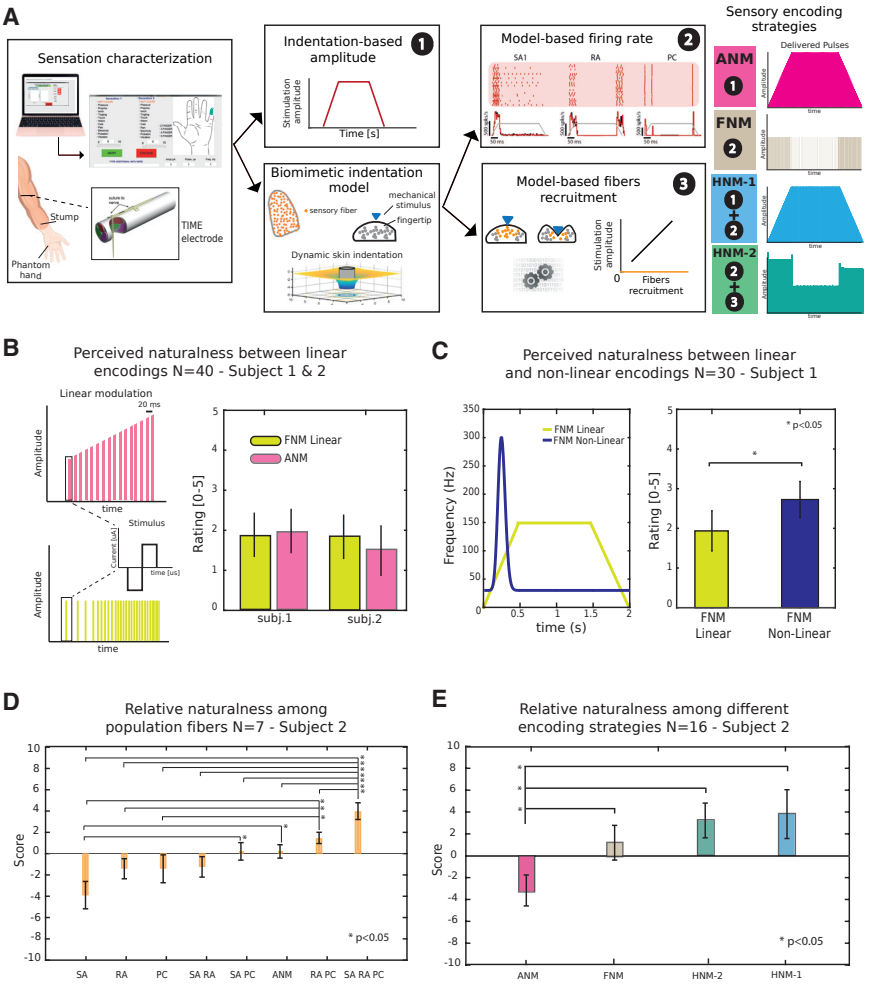

Figure 1. Sensation Naturalness for Different Fibers and Encoding Strategies

For a Figure360 author presentation of Figure 1, see https://doi.org/10.1016/j.neuron.2018.08.033. Figure360▷

(A) Sketch of sensory encoding strategies implemented (ANM, FNM, HNM-1, and HNM-2).

(B) Absolute naturalness perceived using ANM and FNM linear (subjects 1 and 2; 4 active sites; N = 40).

(C) Absolute naturalness perceived using FNM linear and FNM non-linear (subject 1; 3 active sites; N = 30).

(D) Score generated by the relative naturalness comparison among different fiber populations encoding a skin mechanical indentation (subject 2; N = 7 sessions × 28 comparison).

(E) The score is shown among different sensation encoding strategies: ANM, FNM, HNM-1, and HNM-2 (subject 2; N = 16 sessions × 9 comparisons).

Data are represented as average ± SD. Two-tailed Kruskal-Wallis test with Tukey-Kramer correction for multiple groups of data was performed. *p < 0.05.

Figures 1A and S1) on a trans-radial amputee implanted with TIME electrodes (Boretius et al., 2010) (Figures 1A and S1). The frequency neuromodulation (FNM) approach was based on the use of a recent biomimetic model (*TouchSim*) able to reproduce nerve activation patterns of the multifaceted mechanics of the skin and mechano-transduction (Saal and Bensmaia, 2015; Saal et al., 2017). The biomimetic model was used to simulate the response of a peripheral nerve given a pattern of sensory stimuli, and then we used this information for stimulating the nerve to restore sensory feedback. We first compared this encoding strategy with a linear amplitude neuromodulation (ANM) paradigm (Raspopovic et al., 2014), and then with two hybrid neuromodulations (HNMs). The first one (HNM-1) modulates pulse frequency according to FNM and pulse amplitude according to ANM. The second one (HNM-2) modulates pulse frequency according to FNM and pulse amplitude according to the indentation-dependent recruitment of the fibers as simulated by *TouchSim*.

These encoding strategies were compared both in terms of the naturalness of the evoked sensations and in their ability to lead the subjects to discriminate sensory stimuli. Then, we applied these strategies to convert the output of the artificial sensors of a prosthetic hand into stimulation patterns of the peripheral nerve. We assessed both functional performance during a real-life grasping task (Clemente et al., 2016) and the prosthesis embodiment achieved by using the different sensory encoding strategies.

Our findings demonstrate that a hybrid neuromodulation approach based on biomimetic frequency modulation and amplitude modulation represents an effective encoding strategy improving several critical aspects of existing approaches. In fact, this hybrid strategy may provide sensory information that can be felt as more natural (also increasing embodiment), is highly sensitive (allowing recognition of smaller indentations), and can be integrated by the user into the sensorimotor control of a hand prosthesis with tactile sensors.

RESULTS

We first performed in two trans-radial amputees a preliminary characterization of the sensations, evoked by linear modulation of amplitude and frequency of the injected pulses in multiple TIME electrode active sites (Figure 1B). This characterization showed that the two approaches had similar low values on a naturalness scale (Lenz et al., 1993) (Kruskal-Wallis test with Tukey-Kramer post hoc correction [KWTK], $p > 0.2$). Results did not vary across stimulation sites (Figures S2A–S2D). In subject 1, we also tested a nonlinear model of frequency modulation inspired by SA activity (Figures S3A and S3B; STAR Methods for details). This led to an increase in perceived absolute naturalness (Figure 1C; KTWK, $p < 0.05$) over all sites (Figure S2E). As responses elicited by stimulation on different sites were strikingly similar (Figure S2), for the sake of simplicity we chose the most selective

active site, located on a fingertip and evoking a vibration sensation, to test the further encoding strategies in subject 2 (Figure S2E).

Model-Based Frequency Encoding Is Necessary to Provide More Natural Sensations

Then, we compared seven different types of FNMs (SA, RA, PC, SA+RA, SA+PC, RA+PC, and SA+RA+PC) based on the output of the biomimetic model (Saal et al., 2017) on subject 2 to understand how to optimally implement FNM. The model simulates the responses of the three main types of tactile fibers innervating the glabrous skin of the hand (Saal et al., 2017)—slowly adapting type I (SA), rapidly adapting fibers (RA), and vibration-sensitive Pacinian afferents (PC)—to a spatiotemporal stimulus applied to the skin. The mechanical skin indentation (12 mN) was simulated by the model and was encoded by the sole SA, RA, or PC responses or by their combinations. We compared the encoding strategies pairwise: we presented the reference stimulus encoded with one of the seven different types of FNMs, and then with the second one with a 5 s interval and asked the subject which stimulation felt more natural (closer to the sensation felt with the fingertip of the intact limb). We assigned +1 to the winning strategy and −1 to the other. Comparing all the encoding modalities, the SA+RA+PC population elicited the most "natural" perceived sensations with a score of 4 ± 0.7 (KW test, $p < 0.05$; Figure 1D). Combining two different classes of fiber population responses (RA+SA, SA+PC, and RA+PC), the sensation was perceived as more natural than using only one class to convey the indentation information (SA, −4 ± 1.02; RA, −1.5 ± 0.75; PC, −1.5 ± 1.03; SA+RA, −1.4 ± 0.76; SA+PC, 0.5 ± 0.64; RA+PC, 1.5 ± 0.42). In a second paradigm, the same mechanical skin indentation (12 mN) was simulated from the biomimetic model and was encoded by using ANM, FNM, HNM-1, or HNM-2, considering simultaneously SA, RA, and PC fibers (Figures S1 and S4A). The encoding strategies were shown to the subject in pairs and were compared in terms of relative naturalness using the aforementioned protocol. The strategies characterized by the biomimetic frequency modulation (FNM, 1 ± 1.48; HNM-1, 4 ± 2.09; HNM-2, 3.8 ± 1.75) elicited a sensation perceived as more natural than the ANM (−3 ± 1.32) (KWTK, $p < 0.05$; Figure 1E).

Amplitude Modulation Is Necessary to Provide Higher Skin Indentation Sensitivity

The just-noticeable difference (JND) and the point of subjective equality (PSE) (STAR Methods) were calculated for each encoding strategy to assess the tactile ability to discriminate between different stimulation intensities. Systematic changes in modeled indentation force (mN) yielded systematic changes in the evoked percepts, as proven by smooth psychometric functions fitting the data (Figures 2A–2D; likelihood ratio test, $p < 0.05$; Table S2).

Considering single-feature encodings, the tactile JND for ANM was lower than using FNM (12.02 mN versus 26.90 mN, respectively), indicating that the modulation of stimuli amplitude gave higher tactile sensitivity (55.31% decrease of the JND) than modulating frequency. The JNDs in the hybrid encodings were 16.06 mN for HNM-1 and 18.45 mN HNM-2. The JNDs were higher than in ANM, but lower than FNM, indicating that the amplitude modulation of the stimulation trains was crucial for high tactile sensitivity. JNDs were comparable with those found on healthy subjects (King et al., 2010). The Weber fractions, which is the JND divided by the reference value (59 mN), obtained for all the encodings were 0.20 (ANM), 0.45 (FNM), 0.27 (HNM-1), and 0.31 (HNM-2). The PSEs differed by less than 12 mN from the standard (59 mN) in the single-feature and hybrid encodings, reflecting a high discrimination precision. In the encodings in which the stimulation amplitude was modulated (ANM, HNM-1, and HNM-2), there was a tendency to overestimate the stimulus (PSE_{ANM}, PSE_{ANM}, $PSE_{ANM} > 59$ mN). The opposite behavior was observed in FNM encoding ($PSE_{FNM} < 59$ mN).

To assess the discrimination abilities of the subject using the sensory feedback, two discrimination tasks were conducted. First, the subject was asked to distinguish three intensities of skin indentation (low, 11 mN; medium, 59 mN; high, 107 mN) simulated with the biomimetic model and presented randomly. The subject was able to classify the indentation levels above chance (>70% static classification performance [SCP]) with all strategies, indicating some ability to exploit the information encoded in the sensory feedback (Figures 2E and S3C).

Next, the dynamic loading discrimination ability was evaluated. Three different time-varying indentations (dynamic loadings) were presented (increasing, static, and releasing) randomly to the subject. All the encodings allowed the subject to recognize the dynamic indentation trends with high performance (>80% dynamic classification performance [DCP]; Figure S3D), indicating the capability to exploit the encodings in a real-time bidirectional system. In both classification tasks, the functional performance was higher whenever the JND was lower ($JND_{FNM} < JND_{HNM-2} < JND_{HNM-1} < JND_{ANM} \rightarrow DCP_{FNM} < DCP_{HNM-2} < DCP_{HNM-1} < DCP_{ANM}$ and $SCP_{FNM} < SCP_{HNM-2} < SCP_{HNM-1} < SCP_{ANM}$; Figure 3F). Moreover, in the static loading classification task, performances using ANM and HNM-1 were statistically higher than FNM (SCP_{ANM} = 91.6%, SCP_{HNM-1} = 85.7%, and SCP_{FNM} = 70%; Figure 2E; Fisher exact test, $p < 0.05$).

Functional Performance Using Different Sensory Encoding Strategies

The efficacy of different encoding strategies was evaluated during the virtual eggs test (VET) (Clemente et al., 2016). The VET measures the individual's ability to use sensory feedback when the prosthesis is used to lift and transport in a precision grip condition. The subject was asked to transfer as many fragile objects as possible, without breaking them, from one side of an 18 cm tall wall to the other, in 120 s (Figure 3A). The functional performance of the different strategies was compared in terms of manual accuracy, measured as the percentage of unbroken and passed objects with respect to the total number of objects (Clemente et al., 2016), and of gross manual dexterity, measured as the total number of transferred objects (broken and unbroken) (Mathiowetz et al., 1985). All sensory encoding strategies improved the functional performance significantly with respect to the 45% fraction of unbroken passed objects in the no feedback (NF) condition (KW test, $p < 0.05$), but no significant

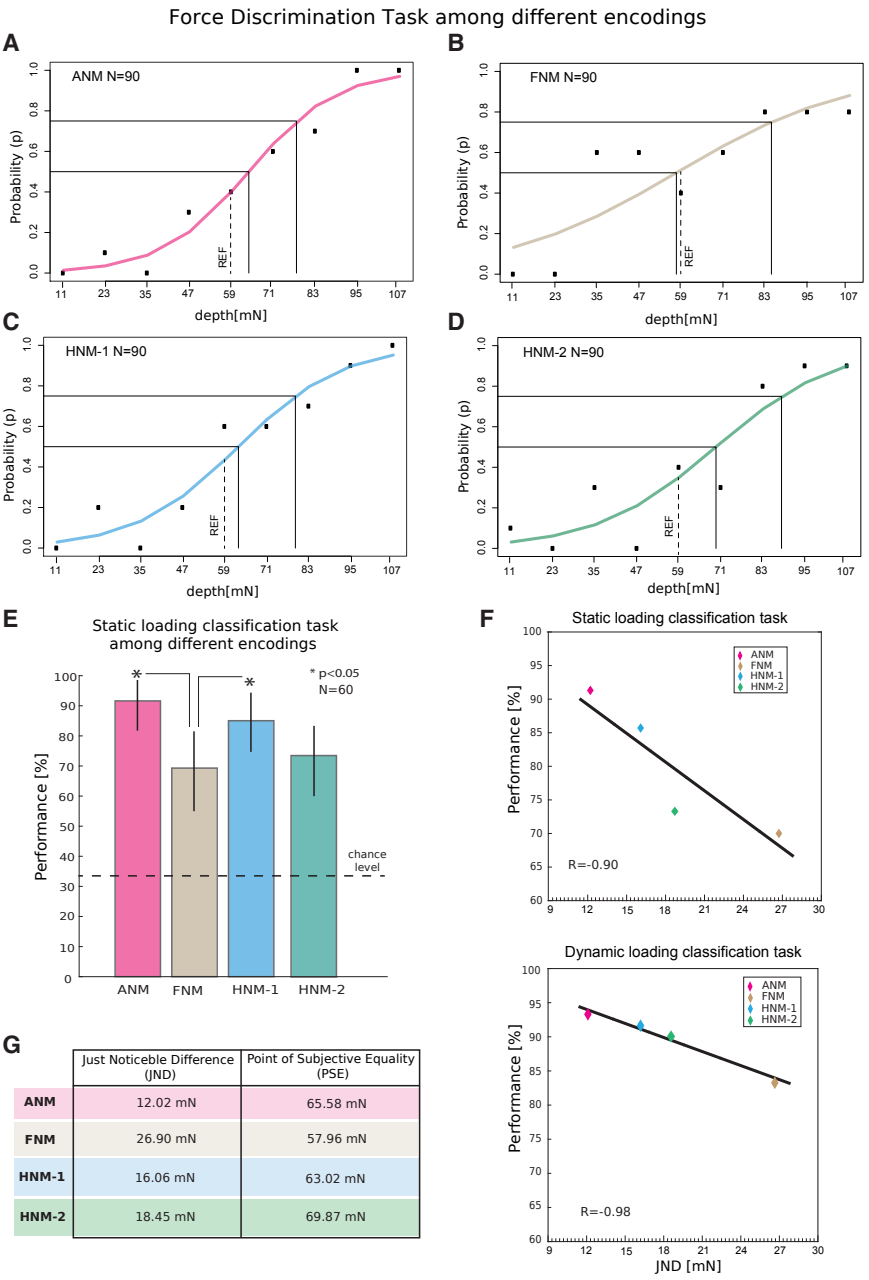

	Just Noticeable Difference (JND)	Point of Subjective Equality (PSE)
ANM	12.02 mN	65.58 mN
FNM	26.90 mN	57.96 mN
HNM-1	16.06 mN	63.02 mN
HNM-2	18.45 mN	69.87 mN

Figure 2. Sensitivity of the Tactile Indentation Discrimination

(A–D) Fitted cumulative Gaussian psychometric functions (filled lines) about the tactile force discrimination according to (A) ANM, (B) FNM, (C) HNM-1, and (D) HNM-2 are shown (N = 90). Dots represent the probability of the indentation presented to be judged stronger than the reference stimulus (59 mN) by the subject. Dashed vertical lines indicate the reference stimulus (59 mN).

(E) Mean and 95% confidence interval of static loading classification task performance (%). *p < 0.05 difference (Fisher exact test).

(F) Correlation between JND (mN) and performance in static (top) and dynamic (bottom) loading classification task performance (%). Tick line indicates linear fitting (R = −0.90 and R = −0.98).

(G) Point of subjective equality (PSE) and just-noticeable difference (JND) are reported for all the stimulation conditions. Only subject 2 ran this test.

differences were observed among the different encoding strategies, all with performances close to 70% (Figure 3B, top inset). In contrast, the gross manual dexterity performance showed significant differences among different encoding strategies (KW test, $p < 0.05$; Figure 3B, bottom inset). Indeed, with both hybrid approaches the subject was able to pass on average 19 blocks, indicating an enhanced gross dexterity compared to single-feature strategies (12.8 and 16.4 blocks for ANM and FNM, respectively) and NF condition (11.6 blocks).

The subject was also asked to answer a questionnaire about the absolute naturalness of the evoked sensation while performing the VET (0, fully unnatural sensation–10, fully natural sensation). Also, two questions regarding the subject's perceptions related to object (Q1 and Q2) were asked (–3, totally disagree; 3, totally agree; STAR Methods). The modulation of the frequency using the biomimetic model (FNM, HNM-1, and HNM-2) was again better in eliciting natural sensations (closer to the sensation felt with the fingertip of the intact limb) than ANM and NF ($score_{FNM,HNM-1,HNM-2} = 5$, $score_{ANM} = 3$, and $score_{NF} < 1$; Figure 3C). Moreover, performing the motor task without any feedback was perceived as less natural (movement not performed like the intact limb, but more artificially) by the subject (score < 1) and the score was statistically different (KW test, $p < 0.05$). Also, the questionnaires related to object manipulation (Q1 and Q2) underlined that the sensory feedback provided more information (Figure 3D). In this case, ANM also yielded similar scores to the biomimetic approaches in terms of perceived quality of the grasp and manipulating information, although it was unable to elicit a natural sensation during the VET ($S_{ANM} < S_{FNM}$; $S_{ANM} < S_{HNM-1}$; $S_{ANM} < S_{HNM-2}$).

Embodiment Is Increased by Natural Sensory Encodings during Closed-Loop Experiments

Psychophysical studies observed that naturalistic and pleasant sensing parameters of tactile stimulations delivered to the intact hand are associated with a stronger embodiment (van Stralen et al., 2014). We then hypothesized that direct neural stimulations leading to a higher relative naturalness of the sensation would also lead to an increased sense of artificial hand/finger ownership. To verify this hypothesis, the rubber hand questionnaire to assess the level of embodiment

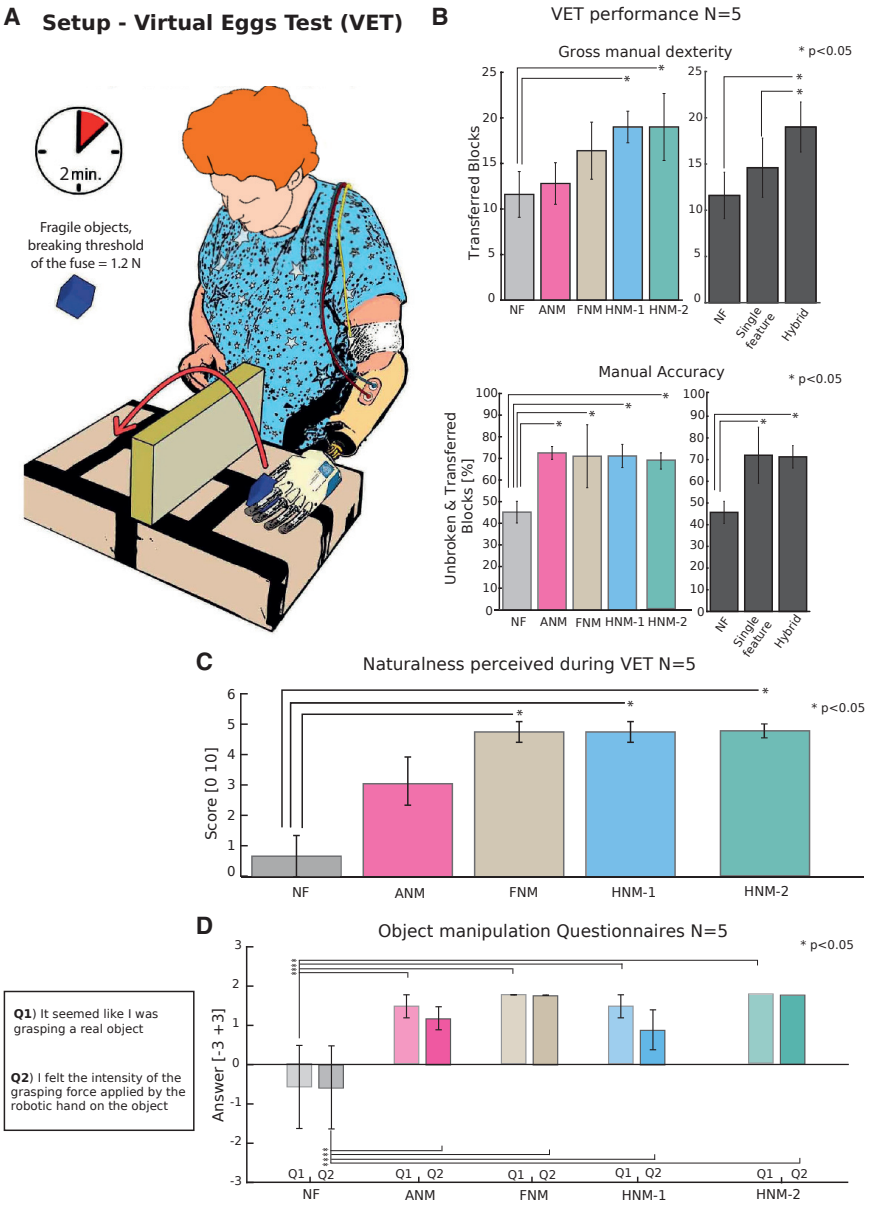

Figure 3. Virtual Eggs Task

(A) Schematic of the virtual eggs task (VET).

(B) Performance in the VET (N = 5 sessions × 5 conditions) in terms of gross dexterity (top) and manual accuracy (bottom). The percentage of unbroken and transferred objects and the number of total transferred blocks among all the sensory feedback modalities are indicated. Data are shown as mean values ± SD.

(C) Absolute naturalness reported by the subject after performing VET on a scale from 0 (fully unnatural) to 10 (fully natural).

(D) Answers to questions regarding the object manipulation ability perceived (Q1 and Q2). Data are reported as average ± SD. Two-tailed Kruskal-Wallis test with Tukey-Kramer correction for multiple groups of data was performed. *p < 0.05. Only subject 2 ran this test.

(Ehrsson et al., 2008; Marasco et al., 2011) while executing the VET was administered (Figure 4). The subject reported the highest embodiment in the conditions in which the sensory feedback was provided, as shown by the significantly higher scores for the three embodiment questions in all the ANM, FNM, HNM-1, and HNM-2 as compared to NF (KW test, $p < 0.05$; Figure 4D). The rubber hand questionnaires confirmed the enhancement of the embodiment when natural sensory encoding was used, as shown by the difference in Q3 score between ANM and FNM, HNM-1, and HNM-2 encodings (KWTK, $p < 0.05$). This explicit answer suggests that, during use, the prosthesis was perceived closer to biological one when more natural encodings were provided. Notably, the illusion questions were rated higher than the control statements (Figure 4E) in all stimulation encodings, thus confirming that the subject was not suggestible (Botvinick and Cohen, 1998; Ehrsson et al., 2008).

Distorted Phantom Limb Perception Is Decreased Using Frequency Model-Based Encodings

We then tested whether a natural encoding used in a closed loop would reduce the distorted perception of the phantom limb, namely, the telescoping effect (Ramachandran and Hirstein, 1998). This perception causes a mismatching of spatial dimensions and posture of the phantom limb. Thus, we quantified abnormal phantom limb perceptions and evaluated the hypothesis that biomimetic encodings reduced telescoping effect after a VET session (Rognini et al., 2018) (Figure 4A). The subject reported her phantom arm length (10 repetitions) before and after each session of VET. She perceived the phantom arm as being distally displaced toward the prosthesis after a single VET session with restored sensory feedback compared to baseline (pre-VET) (Figure 4B). After VET trials without sensory feedback or using ANM or HNM-2, the perceived length of the phantom arm did not change statistically (KW test, $p > 0.05$). Only FNM and HNM-1 showed a statistically significant increase in the perceived length of the phantom arm toward the prosthesis (KW test, $p < 0.05$): the distance between the perceived position of the elbow and the tip of the 5th finger was 19.8 ± 0.6 cm pre-VET and 23.6 ± 0.9 cm post-VET with FNM; 19 ± 0.7 cm pre-VET and 23.7 ± 0.9 cm post with HMN-1. HNM-2 showed a trend in the same direction, but it was not statistically significant. As a reference, intact upper limb measures were as follows: stump length (left) = 10 cm (elbow-tip); arm length (right) = 35 cm (elbow-fingertip). Interestingly, the subject gave a higher score

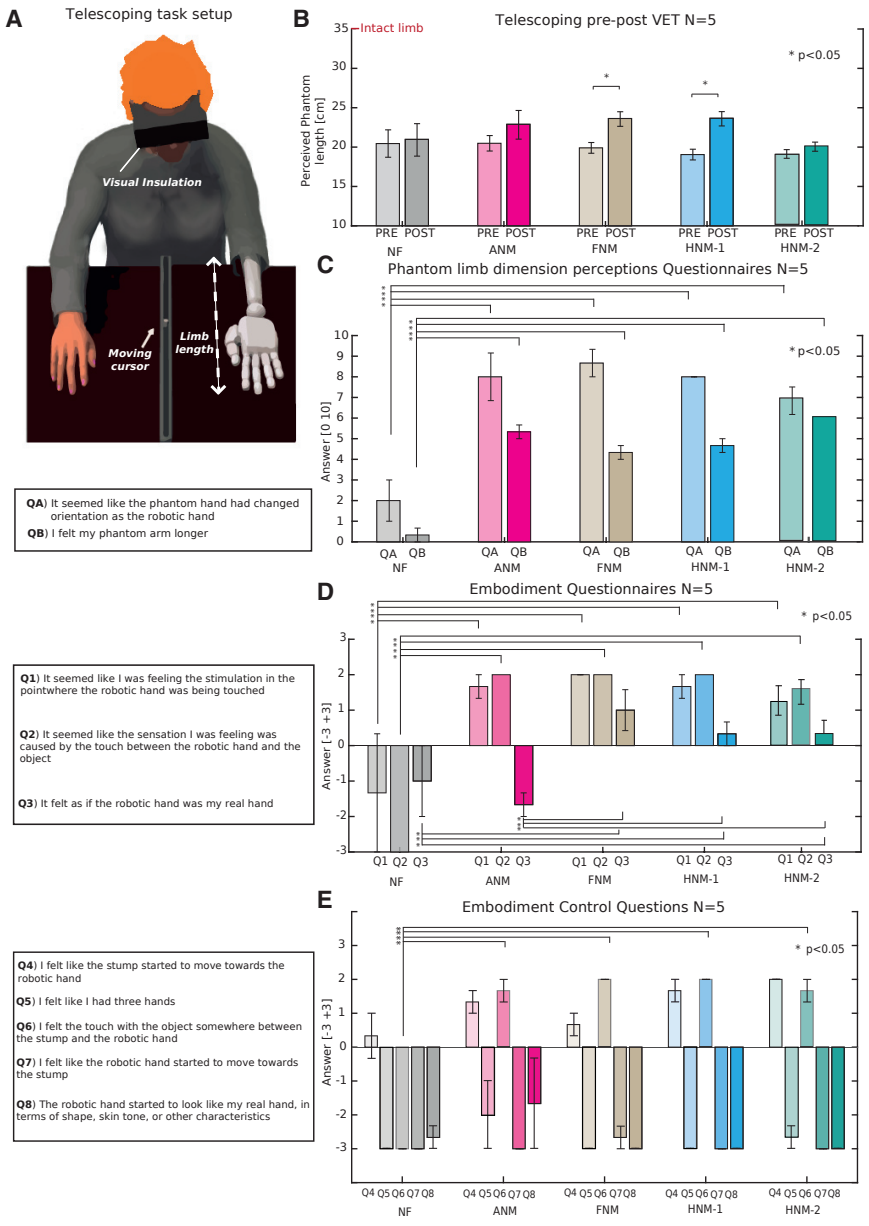

Figure 4. Abnormal Phantom Limb and Prosthesis Embodiment Perception

(A) Experimental setup. The difference between the perceived position of her phantom finger and elbow was used to estimate the perceived length (in cm) of the phantom limb.

(B) Phantom limb length before and after performing the VET (average scores are reported). Two-tailed Kruskal-Wallis test with Tukey-Kramer correction for multiple groups of data was performed. *p < 0.05.

(C) Average answers to questions QA and QB about phantom limb dimension perceptions.

(D) Average ratings of embodiment (Q1–3) after performing VET task.

(E) Control items Q4–8 were rated as with a low rating hand. N = 5 session × 5 conditions. Error bars show SD of the mean. Only subject 2 involved.

in phantom limb dimension perception questions (QA and QB) in all the sensory feedback encodings (Figure 4C). These ratings showed that the use of the bidirectional prosthesis in each stimulation condition (ANM, FNM, HNM-1, and HNM-2) significantly changed the perceived orientation and phantom arm length toward the position of the robotic hand, compared to the NF condition (KW test, $p < 0.05$).

DISCUSSION

The definition of encoding strategies that entail natural and fully exploitable tactile sensations is crucial to improve the acceptability and usability of artificial hands and has not been achieved yet. In this study, we show that the optimal combination of naturalness and sensitivity of the tactile sensory feedback can be achieved with a "hybrid" encoding strategy based on simultaneous biomimetic frequency and amplitude neuromodulation.

Modeling All Mechanosensory Fiber Populations Provides the Most Natural Sensations

We first tested different population makeups in the biomimetic model used for the FNM encoding (only RA, only SA, only PC, or all combinations of pairs or the triplet), and the results indicated that the most natural sensations were achieved when all three fibers populations were included in the model, followed by all the pairs (Figure 1D).

Neural electrodes gradually recruit all the sensory fibers within the fascicle (Oddo et al., 2016; Raspopovic et al., 2017) depending on both distance (threshold proportional to square of distance) and fiber diameter (threshold proportional to 1/square root of fiber diameter). For this reason, each stimulation pulse delivered through these neural interfaces is likely to recruit a mix of RA, SA, and PC sensory afferents present in that fascicle even if clustered (Jabaley et al., 1980). This may explain the more natural sensations obtained when delivering a pulse train able to recruit all three afferent populations rather than skewed toward a specific fiber type (Figure 1D).

Model-Based Frequency Modulation Is Necessary to Provide Natural Tactile Feedback

Encoding approaches including the biomimetic frequency modulation (FNM, HNM-1, and HNM-2) elicited more natural tactile percepts than the amplitude neuromodulation (Figure 1E). Encoding strategies based on linear relationship between stimulation frequency and perceived intensity of the sensory

experience achieved interesting but limited results in terms of sensitivity and naturalness (Graczyk et al., 2016; Tan et al., 2014). Indeed, comparing linear and non-linear FNM (Figure 1C), we found differences in terms of absolute naturalness. This is probably due to the fact that the spectral content associated with skin sensory afferents is much more sophisticated, involving highly stereotyped responses to skin indentation events. To date, biomimetic temporal patterns have been exploited for restoring artificial sensory feedback in a prosthesis only in Oddo et al. (2016) for direct neural stimulation and in Osborn et al. (2018) with non-invasive approaches. However, in both these works only one kind of mechanoreceptor was simulated, while here we simulated the output of the models of three different mechanoreceptors and this led to a larger relative naturalness (Figure 1D).

Amplitude Modulation Is Necessary to Provide Highly Sensitive Tactile Information

Sensory feedback must not only induce sensations that are experienced as more natural, but also convey informative tactile information. Simulating different indentation force encoded by the modulation of amplitude (ANM, HNM-1, and HNM-2) and frequency (FNM, HNM-1, and HNM-2) of the neural stimulation led to a modulation of the perceived sensation intensity. Interestingly, naturalness and indentation sensitivity of encoding strategies were not related, as demonstrated by the JND (Figure 2G). In particular, the presence of an amplitude modulation component in the encoding scheme (ANM and HNM-1) resulted in lower JND value and higher performance during the static loading classification task (Figure 2E), confirming that a higher sensitivity translates into improved function (Figure 2F). In contrast, in the nerve, little information about amplitude is conveyed during sustained responses. Most of the information is conveyed during the transients. Indeed, a similar situation was generated by ANM. In fact, when ANM is used, an increasing number of fibers during the first indentation phase (transient) are activated. Then, during the static phase, the stimulation involves the same number of fibers (since the charge injected does not increase) and they could be less active and could convey little information during sustained responses, similar to the intact limb.

Overall, the innovative technological approach utilized in this study for encoding approaches successfully provided to the subject information about the indentation force, and the observed range of finger sensitivity (JND) was comparable to values obtained in previous experiments measuring psychophysical thresholds for finger interaction on healthy subjects (King et al., 2010).

Hybrid Encoding Strategies Enhance Gross Manual Dexterity and Prosthesis Embodiment

In the functional performance estimation performed by VET, we found that the gross manual dexterity was higher using the hybrid encoding (HNM-1 and HNM-2) rather than single-feature encoding strategies (ANM and FNM), compared to a similar manual accuracy with all strategies (Figure 3B). Our results might indicate that providing natural and highly sensitive tactile information enhances the confidence of the subject, leading to a higher block transfer speed. Indeed, this improvement in sensorimotor control (better gross dexterity with better manual accuracy) suggests that the subject is exploiting a more feedforward control strategy, reducing the cognitive burden.

Unfortunately, due to the limited map of the sensation elicited by the stimulation of different active electrode sites (Figure S2E), we could not provide a somatotopic feedback to the phantom fingers involved in the task, but we only provided feedback to the phantom little finger. More experiments to characterize the relationship between somatotopy and naturalness are necessary and will be performed in the future.

Even in this closed-loop task, the subject reported that injected stimulation induced more natural percepts when using the three model-based approaches (FNM, HNM-1, and HNM-2) than when using simple amplitude modulation (ANM) (Figure 3C), consistent with results in passive stimulation condition (Figure 1E). This indicates that the more natural sensations reported during open-loop stimulation trials are maintained during active prosthesis use. The encoding strategies, which resulted in more natural sensations, also induced a higher sense of prosthesis embodiment (Figure 4D). This indicates that using bioinspired encoding approaches can help prosthesis users incorporate the artificial limb as part of their own body scheme, likely resulting in better prosthesis acceptance (Botvinick and Cohen, 1998; Giummarra et al., 2010).

In addition to higher prosthesis embodiment, two sensory encoding strategies (FNM and HNM-1) resulted in a statistically significant reduction in limb telescoping (Figure 4B). This confirms the usefulness of biomimetic approaches in improving phantom limb sensations associated with prosthesis use (Saal and Bensmaia, 2015).

In conclusion, our results show that sophisticated and biomimetic encoding strategies need to be implemented to provide more natural and useful sensory feedback and open up new opportunities for the extensive use of neuroprosthetic technologies with disabled people.

However, these results need to be confirmed with more subjects. While subjective differences could happen, we believe that the selectivity of fiber recruitment ability as obtained by intraneural electrodes could allow the identification of the best channels usable for each subject to obtain the same type of stable and reproducible results.

STAR★METHODS

Detailed methods are provided in the online version of this paper and include the following:

- KEY RESOURCES TABLE
- CONTACT FOR REAGENT AND RESOURCE SHARING
- EXPERIMENTAL MODEL AND SUBJECT DETAILS
- METHOD DETAILS
  - The biomimetic tactile model
  - Biophysical model of afferent recruitment
  - Modeling linear and non-linear frequency NeuroModulation
  - Modeling biomimetic fibers responses to dynamic skin indentations
  - Assessment of sensation naturalness

SUPPLEMENTAL INFORMATION

Supplemental Information includes four figures and two tables and can be found with this article online at https://doi.org/10.1016/j.neuron.2018.08.033.

ACKNOWLEDGMENTS

The authors are deeply grateful to the subjects who freely donated weeks of their life for the advancement of knowledge and for a better future of people with hand amputation. The authors wish to thank Prof. Sliman Bensmaia for his valuable suggestions during the development and test of the encoding strategies. We also thank Prof. Olaf Blanke for sharing with us the equipment for measuring the telescoping effect and Prof. Stanisa Raspopovic for the valuable discussions during the early phase of the experiments. This work was partly funded by the EU Grant FET 611687 NEBIAS Project (neurocontrolled bidirectional artificial upper limb and hand prosthesis), the National Competence Center in Research (NCCR) in Robotics funded by the Swiss National Q5 Science Foundation, and by the Bertarelli Foundation.

AUTHOR CONTRIBUTIONS

G.V. designed the study and protocols, developed the software and the overall system integration, performed the experiments, analyzed the data, and wrote the paper; F.I. developed the software and the overall system integration, performed the experiments, and analyzed the data; A.M. designed the study, supervised the experiments, and wrote the manuscript; E.D. developed the software and the overall system integration, contributed to experiment design, and wrote the paper; I.S. developed the overall system integration; G.G. selected the subject and managed the regulatory path and clinical aspects; M.C., F.C., and C.C. designed the protocols for the VET, designed and characterized the virtual eggs, and reviewed the manuscript; M.C. and C.C. also developed the robotic hand and force sensors; F.M.P. designed the study, supervised the experiments, and reviewed the manuscript; G.R. designed telescoping experimental setup; T.S. developed the TIME electrodes and delivered technical assistance during implantation and explantation; P.M.R. selected the subjects and was responsible for all the clinical aspects of the study; and S.M. designed the study and protocols, supervised the experiments, and wrote the manuscript. All the authors read, commented on, and approved the manuscript.

DECLARATION OF INTERESTS

F.M.P. and S.M. hold shares of "Sensars Neuroprosthetics Sarl," a start-up company dealing with potential commercialization of neurocontrolled artificial limbs. M.C., F.C., and C.C. hold shares of "Prensilia Srl," a start-up company commercializing robotic hands and assessment tools. The other authors do not have anything to disclose.

Received: May 3, 2018
Revised: July 5, 2018
Accepted: August 22, 2018
Published: September 20, 2018

REFERENCES

Boretius, T., Badia, J., Pascual-Font, A., Schuettler, M., Navarro, X., Yoshida, K., and Stieglitz, T. (2010). A transverse intrafascicular multichannel electrode (TIME) to interface with the peripheral nerve. Biosens. Bioelectron. *26*, 62–69.

Botvinick, M., and Cohen, J. (1998). Rubber hands 'feel' touch that eyes see. Nature *391*, 756.

Bourbeau, D.J., Hokanson, J.A., Rubin, J.E., and Weber, D.J. (2011). A computational model for estimating recruitment of primary afferent fibers by intraneural stimulation in the dorsal root ganglia. J. Neural Eng. *8*, 056009.

Chortos, A., Liu, J., and Bao, Z. (2016). Pursuing prosthetic electronic skin. Nat. Mater. *15*, 937–950.

Clemente, F., D'Alonzo, M., Controzzi, M., Edin, B.B., and Cipriani, C. (2016). Non-invasive, temporally discrete feedback of object contact and release improves grasp control of closed-loop myoelectric transradial prostheses. IEEE Trans. Neural Syst. Rehabil. Eng. *24*, 1314–1322.

D'Alonzo, M., Clemente, F., and Cipriani, C. (2015). Vibrotactile stimulation promotes embodiment of an alien hand in amputees with phantom sensations. IEEE Trans. Neural Syst. Rehabil. Eng. *23*, 450–457.

de'Sperati, C., and Baud Bovy, G. (2017). Low perceptual sensitivity to altered video speed in viewing a soccer match. Sci. Rep. *7*, 15379.

Delgado-Martínez, I., Badia, J., Pascual-Font, A., Rodríguez-Baeza, A., and Navarro, X. (2016). Fascicular topography of the human median nerve for neuroprosthetic surgery. Front. Neurosci. *10*, 286.

Delhaye, B., Hayward, V., Lefèvre, P., and Thonnard, J.-L. (2012). Texture-induced vibrations in the forearm during tactile exploration. Front. Behav. Neurosci. *6*, 37.

Ehrsson, H.H., Rosén, B., Stockselius, A., Ragnö, C., Köhler, P., and Lundborg, G. (2008). Upper limb amputees can be induced to experience a rubber hand as their own. Brain *131*, 3443–3452.

Ernst, M.O., and Banks, M.S. (2002). Humans integrate visual and haptic information in a statistically optimal fashion. Nature *415*, 429–433.

Flesher, S.N., Collinger, J.L., Foldes, S.T., Weiss, J.M., Downey, J.E., Tyler-Kabara, E.C., Bensmaia, S.J., Schwartz, A.B., Boninger, M.L., and Gaunt, R.A. (2016). Intracortical microstimulation of human somatosensory cortex. Sci. Transl. Med. *8*, 361ra141.

Giummarra, M.J., Georgiou-Karistianis, N., Nicholls, M.E.R., Gibson, S.J., Chou, M., and Bradshaw, J.L. (2010). Corporeal awareness and proprioceptive sense of the phantom. Br. J. Psychol. *101*, 791–808.

Graczyk, E.L., Schiefer, M.A., Saal, H.P., Delhaye, B.P., Bensmaia, S.J., and Tyler, D.J. (2016). The neural basis of perceived intensity in natural and artificial touch. Sci. Transl. Med. *8*, 362ra142.

Horch, W., Burgess, P.R., Mei, J., Tuckett, R.P., Carter, K., Ballinger, M., and Poulos, D.A. (1983). The neural signal for skin indentation depth. J. Neurosci. *3*, 14.

Horch, K., Meek, S., Taylor, T.G., and Hutchinson, D.T. (2011). Object discrimination with an artificial hand using electrical stimulation of peripheral tactile and proprioceptive pathways with intrafascicular electrodes. IEEE Trans. Neural Syst. Rehabil. Eng. *19*, 483–489.

Jabaley, M.E., Wallace, W.H., and Heckler, F.R. (1980). Internal topography of major nerves of the forearm and hand: a current view. J. Hand Surg. Am. *5*, 1–18.

Johansson, R.S., and Flanagan, J.R. (2009). Coding and use of tactile signals from the fingertips in object manipulation tasks. Nat. Rev. Neurosci. *10*, 345–359.

Johnson, K.O. (1974). Reconstruction of population response to a vibratory stimulus in quickly adapting mechanoreceptive afferent fiber population innervating glabrous skin of the monkey. J. Neurophysiol. *37*, 48–72.

King, H.H., Donlin, R., and Hannaford, B. (2010). Perceptual thresholds for single vs. multi-finger haptic interaction. In 2010 IEEE Haptics Symposium, 95–99.

Lenz, F.A., Seike, M., Richardson, R.T., Lin, Y.C., Baker, F.H., Khoja, I., Jaeger, C.J., and Gracely, R.H. (1993). Thermal and pain sensations evoked by microstimulation in the area of human ventrocaudal nucleus. J. Neurophysiol. *70*, 200–212.

Manfredi, L.R., Baker, A.T., Elias, D.O., Dammann, J.F., 3rd, Zielinski, M.C., Polashock, V.S., and Bensmaia, S.J. (2012). The effect of surface wave propagation on neural responses to vibration in primate glabrous skin. PLoS ONE *7*, e31203.

Marasco, P.D., Kim, K., Colgate, J.E., Peshkin, M.A., and Kuiken, T.A. (2011). Robotic touch shifts perception of embodiment to a prosthesis in targeted reinnervation amputees. Brain *134*, 747–758.

Mathiowetz, V., Volland, G., Kashman, N., and Weber, K. (1985). Adult norms for the Box and Block Test of manual dexterity. Am. J. Occup. Ther. *39*, 386–391.

Muniak, M.A., Ray, S., Hsiao, S.S., Dammann, J.F., and Bensmaia, S.J. (2007). The neural coding of stimulus intensity: linking the population response of mechanoreceptive afferents with psychophysical behavior. J. Neurosci. *27*, 11687–11699.

Oddo, C.M., Raspopovic, S., Artoni, F., Mazzoni, A., Spigler, G., Petrini, F., Giambattistelli, F., Vecchio, F., Miraglia, F., Zollo, L., et al. (2016). Intraneural stimulation elicits discrimination of textural features by artificial fingertip in intact and amputee humans. eLife *5*, e09148.

Ortiz-Catalan, M., Håkansson, B., and Brånemark, R. (2014). An osseointegrated human-machine gateway for long-term sensory feedback and motor control of artificial limbs. Sci. Transl. Med. *6*, 257re6.

Osborn, L.E., Dragomir, A., Betthauser, J.L., Hunt, C.L., Nguyen, H.H., Kaliki, R.R., and Thakor, N.V. (2018). Prosthesis with neuromorphic multilayered e-dermis perceives touch and pain. Sci. Robot. *3*, eaat3818.

Pasluosta, C., Kiele, P., and Stieglitz, T. (2018). Paradigms for restoration of somatosensory feedback via stimulation of the peripheral nervous system. Clin. Neurophysiol. *129*, 851–862.

Prochazka, A. (2015). Sensory control of normal movement and of movement aided by neural prostheses. J. Anat. *227*, 167–177.

Ramachandran, V.S., and Hirstein, W. (1998). The perception of phantom limbs. The D. O. Hebb lecture. Brain *121*, 1603–1630.

Raspopovic, S., Capogrosso, M., Petrini, F.M., Bonizzato, M., Rigosa, J., Di Pino, G., Carpaneto, J., Controzzi, M., Boretius, T., Fernandez, E., et al. (2014). Restoring natural sensory feedback in real-time bidirectional hand prostheses. Sci. Transl. Med. *6*, 222ra19.

Raspopovic, S., Petrini, F.M., Zelechowski, M., and Valle, G. (2017). Framework for the development of neuroprostheses: from basic understanding by sciatic and median nerves models to bionic legs and hands. Proc. IEEE *105*, 34–49.

Rognini, G., Petrini, F.M., Raspopovic, S., Valle, G., Granata, G., Strauss, I., Solcà, M., Bello-Ruiz, J., Herbelin, B., Mange, R., et al. (2018). Multisensory bionic limb to achieve prosthesis embodiment and reduce distorted phantom limb perceptions. J. Neurol. Neurosurg. Psychiatry. jnnp-2018-318570. Published online August 12, 2018. https://doi.org/10.1136/jnnp- 2018-318570.

Saal, H.P., and Bensmaia, S.J. (2015). Biomimetic approaches to bionic touch through a peripheral nerve interface. Neuropsychologia *79* (Pt B), 344–353.

Saal, H.P., Delhaye, B.P., Rayhaun, B.C., and Bensmaia, S.J. (2017). Simulating tactile signals from the whole hand with millisecond precision. Proc. Natl. Acad. Sci. USA *114*, E5693–E5702.

Schiefer, M., Tan, D., Sidek, S.M., and Tyler, D.J. (2016). Sensory feedback by peripheral nerve stimulation improves task performance in individuals with upper limb loss using a myoelectric prosthesis. J. Neural Eng. *13*, 016001.

Tan, D.W., Schiefer, M.A., Keith, M.W., Anderson, J.R., Tyler, J., and Tyler, D.J. (2014). A neural interface provides long-term stable natural touch perception. Sci. Transl. Med. *6*, 257ra138.

Tan, D.W., Schiefer, M.A., Keith, M.W., Anderson, J.R., and Tyler, D.J. (2015). Stability and selectivity of a chronic, multi-contact cuff electrode for sensory stimulation in human amputees. J. Neural Eng. *12*, 026002.

Tuckett, P., Poulos, A., Horch, W., and Wei, J.Y. (1983). The neural signal for the intensity of a tactile stimulus. J. Neurosci. *3*, 8.

Tyler, D.J. (2015). Neural interfaces for somatosensory feedback: bringing life to a prosthesis. Curr. Opin. Neurol. *28*, 574–581.

Urban, F.M. (1910). The method of constant stimuli and its generalizations. Psychol. Rev. *17*, 229–259.

van Stralen, H.E., van Zandvoort, M.J.E., Hoppenbrouwers, S.S., Vissers, L.M.G., Kappelle, L.J., and Dijkerman, H.C. (2014). Affective touch modulates the rubber hand illusion. Cognition *131*, 147–158.

Wendelken, S., Page, D.M., Davis, T., Wark, H.A.C., Kluger, D.T., Duncan, C., Warren, D.J., Hutchinson, D.T., and Clark, G.A. (2017). Restoration of motor control and proprioceptive and cutaneous sensation in humans with prior upper-limb amputation via multiple Utah Slanted Electrode Arrays (USEAs) implanted in residual peripheral arm nerves. J. Neuroeng. Rehabil. *14*, 121.

Wijk, U., and Carlsson, I. (2015). Forearm amputees' views of prosthesis use and sensory feedback. J. Hand Ther. *28*, 269–277, quiz 278.

Q2 Q3 STAR★METHODS

KEY RESOURCES TABLE

REAGENT OR RESOURCE	SOURCE	IDENTIFIER
Software and Algorithms		
MATLAB R2015b	MathWorks	https://www.mathworks.com
TouchSim	N/A	http://bensmaialab.org
R 3.2.3	R foundation	https://www.r-project.org
Other		
TIME electrodes implant	N/A	N/A
IH-2 Azzurra	Prensilia srl	https://www.prensilia.com
Grapevine Neural Interface System	Ripple LLC	http://rippleneuro.com
Raspberry PI model 3b	Raspberry PI	https://www.raspberrypi.org

CONTACT FOR REAGENT AND RESOURCE SHARING

Further information and requests for resources should be directed to the Lead Contact, Silvestro Micera (silvestro.micera@santannapisa.it).

EXPERIMENTAL MODEL AND SUBJECT DETAILS

Two trans-radial amputees participated in the study. Subject 1 is a 48-years old female with a traumatic trans-radial amputation of the distal third of the left forearm (her dominant hand) occurred 23 years before the enrolment in the study. Subject 2 is a 54-year-old female with a proximal left trans-radial amputation incurred 2 years prior to the study. Nerve ultrasound and later surgery highlighted a reduced cross-section area of the median nerve in the tract between elbow and proximal third of the arm, compared to the physiological values (Delgado-Martínez et al., 2016).

Tests with comparison between ANM and FNM linear (Figures 1B and S2A–S2D) were performed with both subjects. Test with comparison between linear and non-linear FNM (Figures 1C and S2E) were performed with Subject 1. All other tests were performed with Subject 2.

Ethical approval was obtained by the Institutional Ethics Committees of Policlinic A. Gemelli Foundation at the Catholic University, where the surgery was performed. The protocol was also approved by the Italian Ministry of Health. Informed consent was signed. All experiments were conducted in accordance with relevant guidelines and regulations.

Subjects 1 and 2 were recruited in the middle stage of an ongoing long-term study of intraneural TIME implants (respectively 1 and 4 months after implantation). Subject 2 performed all experiments reported here over a period of one month (divided into several sessions) as shown in Table S1A.

METHOD DETAILS

The biomimetic tactile model

The biomimetic model (*TouchSim*) is described in detail in Saal et al. (2017). In general, the model of peripheral afferents is structured in two distinct sequential stages to capture the structure of the mechano-transduction process. First, the deformations experienced by individual receptors given a stimulus applied to the surface of the skin were computed. Then, based on this receptor deformation the spiking response of the nerve fiber using an Integrated-and-Fire (IF) mechanism was calculated.

Biophysical model of afferent recruitment

We estimated the total number of afferents activated by a given mechanical stimulus during time by means of the biomimetic model. The number of active fibers was computed as a function of the distance between the mechanical stimulus and the type of recruited fiber. Moreover, the recruitment of afferents depended on the modeled skin indentation, considering also that a stimulus propagates across the skin and excites afferents whose RFs are located away from the contact area (see Figure S1, top row).

We determined then the amplitude of the electric stimulation (A) over bins of 10 ms as a function of the number of active fibers according to the following equation

$$A(i) = \frac{N(i)_{active\ fibers}}{N_{tot}} * A_{max};, \quad \text{(Equation 1)}$$

where N_{active} fiber (i) is the number of active fibers in 10 ms bin estimated from the model as described above, N_{tot} is the number of total fibers innervating the area (which is again defined by the model) and A_{max} is the maximum amplitude corresponding to a perceived sensation intensity of 8 (in a 0-10 point scale) reported by the subject before each session.

This approach is consistent with previous studies (Bourbeau et al., 2011; Johnson, 1974; Muniak et al., 2007) showing that the recruitment of afferents could be used as a code for sensation intensity.

Modeling linear and non-linear frequency NeuroModulation

ANM (Amplitude NeuroModulation)

Four different active sites (MS-1, MS-2, US-1 and US-2) were used to deliver electrical stimuli to the peripheral nerve where the amplitudes were proportional to the depth of the simulated mechanical indentation. Thus, intraneural stimulation amplitude followed the force indentation profile. The injected trains of biphasic pulses had a fixed frequency of 50 Hz as Raspopovic et al. (2014).

FNM linear (linear Frequency NeuroModulation)

Four different active sites (MS-1, MS-2, US-1 and US-2) were used to deliver electrical stimuli to the peripheral nerve where the frequency was proportional to the force of the simulated mechanical indentation. Thus, intraneural stimulation frequency followed the indentation profile. The injected charge had a fixed value (medium between perceptual threshold and below pain value) for each active site used.

FNM non-linear (non-linear Frequency NeuroModulation)

Three different active sites (MS-1, MS-2 and US-1) were used to deliver electrical stimuli to the peripheral nerve where the frequency followed a non-linear envelope (Figures S3A and S3B) similar to the SA fiber response to a mechanical indentation. The injected charge had a fixed value (medium between perceptual threshold and below pain value) for each active site.

Modeling biomimetic fibers responses to dynamic skin indentations

The mechanical simulated stimulus was defined as the time-varying positions of a 100 μm radius pin (corresponding to a circular probe) indenting into the skin orthogonally to its surface. The contact location used in all experiments was fixed as the fingertip of the 5th finger (Figure S1), since the subject referred the sensation evoked by the neural stimulation in that precise location (Figure S2E). Thus, a ramp stimulus with different forces (mN), according to the task, has been presented. The temporal structure of the mechanical stimulus was fixed to 2 s (500 ms of rise, 1 s of static and 500 ms of release). The stimulus was encoded using different strategies (see below) and converted to commands for the neurostimulator. Figure S1 schematically present the processing steps performed to generate all the sensory encodings. In all cases, the intraneural stimuli were delivered as trains of charge-balanced, cathodic-first, biphasic and symmetric square-shape current pulses of variable intensity and frequency according to the encoding type, through a dedicated software controlling the external electrical stimulator (Ripple Grapevine LLC).

FNM (Frequency NeuroModulation)

After simulating the dynamic skin indentation, we generated the responses of the fibers SA, RA and PC separately using the biomimetic model. The spikes generated by the fibers were then summed to get the overall spiking activity. The population firing rate was computed counting the spikes from all fibers in bins of 10 ms. Then, for each bin, the pulse frequency (in Hz) of the stimulation was set as the population firing rate. By doing so, the electric stimulation maintained the frequency structure/profile of the neural fiber population responding to a mechanical skin indentation. Using this approach, the fibers population response generated by the model was changed according to the modeled indentation force (taking into account also its velocity and acceleration), mimicking the natural coding. Thus, the frequency of intraneural stimulation encoded the biomimetic population firing rate (i.e., the frequency of stimulation was set equal to the frequency of spiking of the biomimetic fibers population).

The amplitude of the stimuli injected was fixed as that value at which the subject perceived a medium (5 in a scale between 0 (no sensation) and 10 (before to be painful)) sensation intensity ($[A_{max}\text{-}A_{min}]/2$, where A_{max} = upper sensation limit and A_{min} = sensation threshold at f = 50 Hz and t_{pw} = 60 μs).

ANM (Amplitude NeuroModulation)

An active site was used to deliver electrical stimuli to the peripheral nerve where the amplitudes were proportional to the depth of the simulated mechanical indentation. Thus, intraneural stimulation amplitude followed the force indentation profile. The injected trains of biphasic pulses had a fixed frequency of 50 Hz as Raspopovic et al. (2014).

HNM-1 (Hybrid NeuroModulation-1)

The hybrid approaches were generated by the simultaneous modulation of frequency and amplitude of the intraneural stimulation. In this case the stimulation frequency was defined based on the biomimetic model of the responses of SA, RA, PC fibers, predicted by the biomimetic model, summed to get a population firing rate (see above, subsection FNM). The amplitude of the stimulation was proportional to the modeled indentation force as (see above, subsection ANM). This created a hybrid model in which we modulated frequency according to the biomimetic model and the amplitude according to the proportional scheme.

HNM-2 (Hybrid NeuroModulation-2)

This approach consists in the conversion of the mechanical skin indentation using the population fibers firing rate and recruitment simultaneously. The first parameter was generated as in FNM using all the fibers types and the number of recruited fibers was estimated by the biomimetic model counting the activated fibers. Then, the population firing rate in response to the stimulus was converted in frequencies of stimulation trains injected and the fibers recruitment during the indentation in amplitudes following Equation 1.

For the typical timescales involved in our experiments (in the order of seconds), the subject did not report relevant changes in sensation duration or strength, which should indicate the absence of adaptation. For all practical purposes, adaptation was insignificant during our experiments.

Assessment of sensation naturalness

We first characterized the subjects' rating of the perceived naturalness of the stimulation delivered through TIMEs. We injected biphasic trains of current pulses lasting 2 s with an increasing phase (0.5 s), a static phase (1 s) and a decreasing phase (0.5 s) (Figure S1, top row, and 1B) using ANM or linear FNM, through 4 active sites of the electrodes (2 on median and 2 on ulnar nerve). The subjects were asked to report the location, type and naturalness, rated on a scale from 0 to 5 (Lenz et al., 1993). Four active sites of the median and ulnar nerves implanted electrodes (Figures 1B, 1C, and S2A–S2D) were tested (N = 40).

With Subject 1 we tested the same paradigm comparing FNM linear to FNM non-linear, generated based on the SA response (Figures S3A, S3B, and S2E) with three different active sites.

A set of 7 different populations of fiber activities in response to a skin indentation force of 12 mN depth was designed for FNM. The set contained all the possible combinations of the 3 different fiber types: SA, RA and PC. All fibers had their receptive field in the middle of the last phalanx of the 5th finger, as shown in Figure S1. The ANM was used as a reference because of its extensive use in a previous study (Raspopovic et al., 2014). Two different ramp of skin indentations with 2 s length and 12 mN depth (encoded by the different approaches) were presented to the subject, one after the other in random order, separated by 5 s (two-interval forced-choice scheme) (Ernst and Banks, 2002). The subject was asked to assess which one was the most natural in terms of sensation quality. When the subject rated a stimulus as more natural, 1 point was assigned to that fiber population and -1 point to the other populations. For stimuli perceived with the same naturalness, no point was assigned to both population types. Thus, for each population, the total scores were calculated as the sum of all the points collected during the experiment. A total of 196 (28 comparisons x 7 sessions) trials were performed. The fibers population resulting in the higher score was used as the base for the generation of the intraneural stimulation in all the following experiments.

The fibers population being fixed, a comparison between the four types of encoding strategies (ANM, FNM, HNM-1 and HNM-2) was performed. The same stimulus used in the previous experiment was used in this case as well. Two stimuli were delivered to the subject, sequentially and in a random order, who was asked to report which of the two was perceived as more natural. The same scoring method used in the previous task was exploited also in this case. In this case, a total of 144 comparisons (9 pairs x 16 sessions) were performed. The subject was blinded to the sensory encodings used in each trial. A scale of relative naturalness according to different encoding strategies is shown in Figures 1D and 1F.

Skin indentation discrimination

In order to understand which encoding strategy is optimal in terms of indentation sensitivity (mN), different levels of indentation of the mechanical skin were simulated and compared in a psychophysical experiment. A pair of simulated skin indentations was presented to the subject (encoded by two consecutive trains of stimulation), who was asked to report which one was stronger. The indentation difference between two stimuli was dimensioned after a pilot study. In this, the subject was asked to judge different perceived indentation forces (which one was the stronger) compared to a reference 12 mN indentation (N = 80 repetitions). Since the lowest performance (around 60%) were achieved already for 23 and 35 mN, 12 mN was chosen as a depth step to use. Also, this step was already used in previous studies (Horch et al., 1983; Tuckett et al., 1983).

We chose 9 modeled indentation forces (from 11 mN to 107 mN) of 2 s, which were used in an experimental paradigm exploiting the method of constant stimuli (Urban, 1910) in order to find the JNDs, using a stimulus of 59 mN indentation force as the reference. Each experimental block comprised 90 repetitions, and the subject was given a break between blocks. In each block, each stimulus pair was presented 10 times, and both the order of stimuli within the pair and the order of the pairs was pseudorandomized. The two pulse trains lasted 2 s and were separated by a 4 s inter-stimulus interval. The subject was instructed to ignore any changes in duration or location of the sensations if such changes were to occur and to focus solely on the perceived modeled indentation force (intensity). The subject was blinded to the particular sensory encodings of each trial.

Maximum likelihood estimation was used to fit a cumulative Gaussian and the Point of Subjective Equality (PSE) (de'Sperati and Baud Bovy, 2017), the 75% discrimination threshold (or Just-Noticeable Difference, JND) (Flesher et al., 2016; Graczyk et al., 2016) and the standard deviation of the Gaussian probability distribution were calculated (Ernst and Banks, 2002). The discrimination threshold gives the indentation difference perceived between the 59 mN and another indentation that elicited 75% of correct response. It is directly related to the standard deviation σ of the underlying Gaussian $JND_{0.75} = z_{0.75}\,\sigma$ where $z_{0.75} = 0.6745$ is the quantile of the standardized Gaussian probability distribution corresponding to 75%. A likelihood ratio test was conducted to verify

the goodness of psychometric curve fitting. Moreover, to compare discriminability across sensory encodings, the Weber fraction, which is the JND divided by the reference value (59 mN), was computed (Graczyk et al., 2016).

Biomimetic model-based neuroprosthesis

The closed-loop system included a robotic hand with tactile sensors, controlled by the subject using sEMG signals, along with a controller and a neural stimulator, implementing the encoding strategies and providing sensory feedback in real time by means of implanted TIMEs (Boretius et al., 2010). For the firing rate model-based approaches (FNM, HNM-1 and HNM-2), the corresponding frequency trains were computed previously offline by the model to reach the appropriate speed during the real-time implementation. During the experiments reported in this work, a single tactile channel was used for sensory feedback in all the conditions and across days. Each day we verified that the neural stimulation was still comfortable and identical to the previous sessions. The parameters were chosen in a way to optimally cover the whole dynamic range of sensations reported by the subject, and were able to induce the stable and reproducible sensations across all sessions. Indeed, the dynamic range of the hand sensor was mapped and divided using the JND information with steps of 12.06 mN in ANM, 26.90 mN in FNM, 16.06 mN in HNM-1 or 18.45 mN in HNM-2 according to the encoding type used. In that way, the stimulation values were computed for frequency and amplitude of the stimulation train in real time according to sensor values, conveying its sensory information to the subject. Each tactile encoding algorithm, used to transfer the model output in the sensory feedback, provided by the bidirectional hand system was reported in detail in the following subsections (Bidirectional system and tactile encoding algorithms).

The delivered charge was modulated differently in ANM, HNM-1, HNM-2, and FNM, but the same range (12 to 18 nC; Figure S4A) in all the conditions was considered. For ANM, the range used was 12nC to 18nC, where the amplitude was modulated (between 200 μA and 300 μA) and the pulse-width was fixed to 60 μs (and f = 50 Hz). In this case, as in HNM-1, the amplitude followed the profile of the stimulus (Figure 1). For FNM, the charge was fixed to 15 nC (250 μA and 60 μs), middle point of the ANM and HNM-1 range. For HNM-2, the range of charges used was equal to ANM and HNM-1 (12-18 nC), the only difference was the modulation profile which was proportional to the number of activated fibers generated by the biomimetic model.

Virtual Eggs Test (VET) set-up and assessment

The VET is a recently proposed test for sensorimotor assessment (Clemente et al., 2016). In brief, it is a modification of the well-known box and blocks test except that fragile/breakable blocks (resembling virtual eggs) are used instead of the standard wooden ones. During the VET, the subjects are instructed to transfer the fragile blocks presented in front of her from one side to the other of an 18 cm tall wall as fast as possible but without breaking them (Figure 3A). The performance was measured by the number of blocks transferred and the percentage of blocks broken during 2-min trials, akin to the standard box and blocks test. In this work the virtual eggs (40x40x40 mm blocks, ~80 g) exploited a magnetic fuse mechanism which would collapse/break when grasped with a grip force (GF) larger than a specified threshold. The latter was calibrated at a force value that was roughly 10% larger the grip force required by the artificial hand to lift it (1.23 ± 0.02 N).

The protocol included 5 sessions, 5 trials per session, in which the subject grasped the blocks with a tripod grip (thumb, index, and middle finger). Force sensors measured the force applied by the middle finger during grasp. The readout of the sensor was converted into neural stimulation according to the encoding strategies FNM, ANM, HNM-1, HNM-2 and NF (No sensory Feedback provided). Different strategies were presented in a randomized order within and among sessions. The subject was blinded to the particular sensory encoding of each session. To determine if the number of broken blocks was affected by different feedback strategies, we computed the percentages of the number of unbroken blocks transferred and the number of total objects transferred in the FNM, ANM, HNM-1, HNM-2 and NF conditions with N = 25 (5 sessions × 5 trials).

Moreover, the subject was asked to rate the sensation absolute naturalness during the functional task giving a score from 0 (completely unnatural) to 10 (as done with my healthy hand). In particular, three questions were asked to the subject, after the VET, in order to assess the object manipulation ability perceived (Q1- 'It seemed like I was grasping a real object' and Q2- 'I felt the intensity of the grasping force applied by the robotic hand on the object'). The subject was asked to report the agreement to the questions using a scale ranging from −3 (absolutely disagree) to 3 (absolutely agree).

Prosthesis embodiment questionnaire

The questionnaire was adapted based on previous studies investigating the sense of body ownership in amputee subjects (D'Alonzo et al., 2015; Marasco et al., 2011). The first three questions were designed to assess the strength of the illusion. The 5 other questions, unrelated to the illusion, served as control for suggestibility (Figure 4E). The subject was required to rate the extent to which these questions did or did not apply to their current experience using a scale ranging from −3 (absolutely certain that it did not apply) to 3 (absolutely certain that it did apply). AS the questionnaire followed each trial of the VET, a total of 25 questionnaires were collected.

Telescoping effect measurement

The subject integration of the prosthesis in the body image was assessed through objective and subjective measures, i.e., a telescoping effect measurement and a questionnaire, respectively. In particular, we developed a set-up to experimentally assess whether the tactile encoding was effective in reducing abnormal phantom hand perceptions. To measure the subject's perceived phantom limb length, we placed a ruler with a movable cursor to the right of the subject's amputated arm. The subject could operate

the cursor with her right hand to indicate the location where she perceived the tip of her phantom 5th digit and the tip of her elbow (Figure 4A). The telescoping measurements were performed 10 times (with randomized finger and elbow assessments) before and after the VET trials. This sequence was repeated 5 times per condition (in random order), resulting in a total of 50 measurements per condition *before* VET and 50 measurements per condition *after* VET.

At the end of each condition, immediately before the 5-min break, we also asked to rate how she perceived the phantom limb at that moment answering to two questions (QA-'It seemed like the phantom hand was changed orientation as the robotic hand' QB-'I felt my phantom arm/hand longer') on a scale ranging from 0 (completely disagree) to 10 (completely agree).

Skin mechanical model

The skin mechanical model used in *TouchSim* is described in detail in Saal et al. (2017). In the model the skin is assumed to be a homogeneous, isotropic, elastic half space, and the stimulus (spatiotemporal pattern of indentation) is applied at the free border of this half-space. The pin is considered to be frictionless and produces load only in perpendicularly to the skin. Considering the responses of whole populations of afferents in quasi-real time, the model not attempt to estimate the exact deformation state of the finger but, simplified the issue by assessing two quantities that are strongly associated with neural response. The local vertical stress based on a quasi-static elastic model of the skin, mainly affecting receptor responses at low frequencies (< 100 Hz) (Delhaye et al., 2012) and dynamic variations in pressure propagated across the skin as surface waves, mainly affecting receptor responses at higher frequencies (Delhaye et al., 2012; Manfredi et al., 2012). These two quantities are then combined in the spiking model and differentially weighted depending on afferent type — slowly adapting type I (SA), rapidly adapting fibers (RA), and vibration-sensitive Pacinian afferents (PC)—.

Mechanical indentation stimuli

The *TouchSim* model accepts as input to describe the mechanical stimulus, a temporal indentation trace together with the radius of the pin that will press on the finger generating the indentation; the radius of the pin has been fixed to 100 μm to evaluate the sensation when pressing on a flat surface on the 5th finger. The indentation depth profile is converted to an indentation force profile. All the traces fed into the model were summed with a sinusoid with 0.12 mN amplitude and 50 Hz frequency, as vibrational noise.

Psychometric fitting

The proportion of trials in which participant evaluated the comparison stimulus to be stronger than the standard thus varied as a function of the physical difference between standard and comparison stimuli. This probability distribution of discrimination responses is modeled mathematically as a function of the physical difference between standard and comparison stimuli, the so-called psychometric function (Figures 2A–2D). The parameters that define the shape of the psychometric function characterize perceptual performance, e.g., the difference in mechanical skin modeled indentation force necessary for participant to reliably discriminate two indentations. Perceptual discrimination performance is modeled by fitting a cumulative Gaussian function with two free parameters (midpoint μ and standard deviation σ) to the responses of the 2AFC indentation discrimination task (Skin indentation discrimination). The Method of Constant Stimuli as the simplest and least biased method to measure a complete psychometric function. In this method, the participant compares the standard stimulus (59 mN) to comparison stimuli (from 11 mN to 107 mN) drawn from a fixed set of modeled indentation forces for a fixed number of repetitions. A cumulative Gaussian function describing an 'S'-shape (Figures 2A–2D) results from summing up (integrating) the values of a bell-shaped Gaussian function. The σ parameter of the psychometric function corresponds to the distance x between the points of the psychometric function at which 0.5 and 0.75 correct responses are reached. This value relates inversely to the slope of the psychometric function at 0.5. It is called the Just Noticeable Difference (JND) and is inversely related to the cue reliability. The parameter μ of the psychometric function defines the Point of Subjective Equality (PSE), i.e., the stimulus value that corresponds to the point 0.5 of the psychometric function.

Q4

Intraneural stimulation parameters

The active site chosen for this study was R5 of the electrode 3 implanted in the distal part of the ulnar nerve. The sensation reported by subject was a vibration of the 5th figertip. The range of stimulation amplitude used was from 200 μA to 300 μA for ANM, HNM-1 and HNM-2 and fixed to 250 μA for FNM. The intraneural stimulation train frequency was fixed to 50 Hz for ANM or spaced from 1Hz to 1kHZ in model-based frequency strategies (FNM, HNM-1 and HNM-2). Instead, the pulse width was fixed to 60 μs for all the stimulation conditions (Table S1B). The injected charge of 18 nC was far below the safe level of 120 nC for the stimulation sites (Boretius et al., 2010).

Static loading classification task

In order to demonstrate that the participant could effectively and reliably discriminate the sensory feedback associated to different modeled indentation forces without a comparison (as in method of constant stimuli) an experiment was designed and carried out according to all the encodings. The subject performed the task (N = 3 stimuli x 20 repetitions x 4 encodings) blindfolded and acoustically isolated. She did not receive any systematic and prolonged training. During the force discrimination task, the subject was instructed to recognize three different simulated modeled indentation forces generated by the biomimetic model randomly delivered by the experimenter. The subjects had to declare the perceived modeled indentation force by voice. The modeled indentation forces

were: low, medium and high indentation of the 5th finger. Finally, we compared the performance in the task, when intraneural stimulation was provided using all the tactile encoding strategies. The indentation force traces were designed as a ramp going up from 0 mN to the defined depth in 0.5 s, followed by a plateau of 1 s and a decreasing ramp to 0 mN again in 0.5 s (Figure S1, First Step); the three selected forces where 12 mN for the low indentation, 59 mN for the medium and 107 mN as the high one.

Dynamic loading classification task

For the dynamic loading classification task, the subject was instructed to discern three indentations with different temporal structure using only the sensory feedback provided. These stimuli were randomly shown by the experimenter. The subject had to indicate the dynamic structure of the perceived indentation by voice. The indentations provided were: penetrating, static and releasing indentation. The subject performed the task (N = 3 stimuli x 20 repetitions x 4 encodings) blindfolded and acoustically isolated. Then, we compared the performance in the task, when intraneural stimulation was provided using all the tactile encoding strategies. All the three indentation traces started with 0.5 s at a fixed depth of 59 mN, followed by a ramp going up to 107 mN simulating a penetrating indentation, going down to 107 mN for a releasing indentation and remaining at 59 mN in the static indentation case for 2 s.

Bidirectional system and tactile encoding algorithms

Subject was fitted with a custom bidirectional prosthesis, allowing control of hand opening and closing by processing surface electromyographic (sEMG) signals, and providing sensory feedback by means of electrical stimulation of the peripheral nerves using TIME. A robotic hand with pressure sensors integrated within each finger (Prensilia Azzura IH2, Prensilia, Italy) was controlled using a custom, multithreaded C++ software running on a RaspberryPi 3 single board computer (Raspberry Pi Foundation, UK). A recording and stimulating device (Neural Interface Processor, Ripple LLC, US) was also connected to the central single board computer, acquiring sEMG data from four bipolar channels, and providing stimulation outputs to one of four neural electrodes. The instance with acquisition, recording and encoding lasted 100 ms. Custom molded sockets were built with integrated screws to easily fix the robotic hand on the end. Holes were drilled in the appropriate positions to allow for the placement of sEMG electrodes on the stump.

Different levels of indentation have been chosen, based on the JND for each encoding strategies, the indentation traces had a constant temporal structure at the given stimulus. Indeed, we mapped the range of the sensor with a step equal to the JND. The model spike trains generated by the combination of SA, RA, and PC at the center of the indentation were sampled at 50 Hz, cropped at 1000 Hz because of the physical limit of the stimulator. For calculating the recruitment, the population activity of the fibers was sampled every 20 ms and the number of active fibers was stored. This number was used to scale between the minimum and maximum amplitude safety level. First, the model data of frequencies and amplitudes for the stimulation trains to inject were sent to the system controller of the bidirectional hand. Here, the range of the force hand sensor based on JNDs was re-mapped. Finally in real time, the force applied by the subject was converted to the pre-defined set of parameters (frequency and amplitude) generated by the model.

For ANM, the measured force applied by the prosthetic digits was encoded using a linear amplitude modulation scheme (Raspopovic et al., 2014), designed to associate perceived stimulation intensity with measured hand force.

Prosthesis hand control

In Virtual Eggs Task (VET) the subject intuitively controlled the bidirectional hand prosthesis using the residual muscle activity. To this aim, four bipolar channels of sEMG were acquired from forearm residual muscles, where palpation was used to place the electrodes in the optimal positions. A three classes (open, close, rest) KNN (k = 3) classifier was implemented and used by the subject (Prochazka, 2015). The sEMG data was acquired with a sampling frequency of 2 kHz and filtered using an IIR filter with 4th order Butterworth characteristics, between 15 and 375 Hz, as well as a notch filter to remove 50 Hz power hum and the harmonics at 100 Hz and 150 Hz. The waveform length (WL) was computed in real time over a window of 100ms for each channel. The WL controlled hand actuation speed (proportional control) updating the value every 100ms.

QUANTIFICATION AND STATISTICAL ANALYSIS

Statistical analysis

All data was analyzed using MATLAB (R2016b, The Mathworks, Natick, US) and R (version 3.2.3, R Development Core Team). All statistics were performed using the available built-in functions. A one-sample Kolmogorov-Smirnov test was used to determine if the datasets associated with the various experiments were normally distributed. None of our datasets passed the test. We therefore used non-parametric alternatives (Kruskal-Wallis (KW) instead of Anova) and reported the average and standard deviation. All reported p-values resulting from Kruskal-Wallis tests measure the significance of the chi-square statistic. When appropriate, multi group correction was applied using Tukey's Honestly Significant Difference Procedure. A Kruskal-Wallis test was computed to show if the VET functional performances were different among encodings. A multiple comparison correction was applied. Performances that were found to be statistically different are marked with a star ($p < 0.05$). Additional details about the number of repetitions for each experiment are reported in the corresponding figure legends. When random numbers were needed (e.g., generating object presentation sequences), random permutations of an equi-populated sequence were used.

DATA AND SOFTWARE AVAILABILITY

The datasets generated during and/or analyzed during the current study are available from the corresponding author on reasonable request.

ADDITIONAL RESOURCES

This study was conducted as part of the clinical NCT02848846 (https://clinicaltrials.gov/).